On the critical flame radius and minimum ignition energy for spherical flame initiation

Zheng Chen [a,*], Michael P. Burke [b], Yiguang Ju [b]

[a] *State Key Laboratory for Turbulence and Complex Systems, Department of Mechanics and Aerospace Engineering, College of Engineering, Peking University, Beijing 100871, China*
[b] *Department of Mechanical and Aerospace Engineering, Princeton University, Princeton, NJ 08544, USA*

Available online 7 August 2010

Abstract

Spherical flame initiation from an ignition kernel is studied theoretically and numerically using different fuel/oxygen/helium/argon mixtures (fuel: hydrogen, methane, and propane). The emphasis is placed on investigating the critical flame radius controlling spherical flame initiation and its correlation with the minimum ignition energy. It is found that the critical flame radius is different from the flame thickness and the flame ball radius and that their relationship depends strongly on the Lewis number. Three different flame regimes in terms of the Lewis number are observed and a new criterion for the critical flame radius is introduced. For mixtures with Lewis number larger than a critical Lewis number above unity, the critical flame radius is smaller than the flame ball radius but larger than the flame thickness. As a result, the minimum ignition energy can be substantially over-predicted (under-predicted) based on the flame ball radius (the flame thickness). The results also show that the minimum ignition energy for successful spherical flame initiation is proportional to the cube of the critical flame radius. Furthermore, preferential diffusion of heat and mass (i.e. the Lewis number effect) is found to play an important role in both spherical flame initiation and flame kernel evolution after ignition. It is shown that the critical flame radius and the minimum ignition energy increase significantly with the Lewis number. Therefore, for transportation fuels with large Lewis numbers, blending of small molecule fuels or thermal and catalytic cracking will significantly reduce the minimum ignition energy.
© 2010 The Combustion Institute. Published by Elsevier Inc. All rights reserved.

Keywords: Spherical flame initiation; Critical flame radius; Minimum ignition energy; Lewis number

1. Introduction

Flame initiation is one of the most important problems in combustion research and it plays an important role in the performance of combustion engines. Understanding flame initiation is therefore not only important for fundamental combustion research but also essential for better control of fuel efficiency, exhaust emissions, and idle stability in engine operation. It is well known that successful ignition depends on the amount of energy in the form of heat and/or radicals deposited into a combustible mixture. If the energy is smaller than the so-called minimum ignition energy (MIE), the resulting flame kernel decays rapidly because heat/radicals conducts/diffuse away from the kernel and the dissociated species recombine faster than they are generated by chemical reactions within the

* Corresponding author. Fax: +86 10 6275 7532.
E-mail address: cz@pku.edu.cn (Z. Chen).

ignition kernel [1–4]. Furthermore, experiments [5–7] and simulations [23,24,29,30] (see also references in Ref. [1]) demonstrated that there is a critical flame radius for spherical flame initiation such that flame kernels that can attain this critical radius result in successful ignition. Despite extensive research effort over many decades on flame initiation, it remains unclear what length scale (i.e. the critical flame radius) controls flame initiation and how it is related to the MIE.

In the classical thermal-diffusion theory, the minimal radius of the developing flame kernel for successful flame initiation was related to the quenching distance or the flame thickness [2–4]. To explain their measurements of the MIE for different mixtures, Lewis and von Elbe [2] proposed that the spark heated the surrounding mixture and ensured continued flame propagation. The minimum size of this heated "spark kernel" was thought to be related to the quenching distance or the flame thickness, such that the MIE was postulated to be the spark energy necessary to heat the kernel to the adiabatic flame temperature [2]. Similarly, based on the thermal-diffusion theory, Zeldovich [4] proposed that the critical length controlling spherical flame initiation was the flame thickness such that the MIE was proportional to the cube of the flame thickness.

Unfortunately, the above models could only phenomenologically describe the spark ignition since fuel consumption and thus mass diffusion were not considered. A more accurate description of flame ignition that included the effect of preferential diffusion of heat and mass (i.e. the Lewis number effect) was proposed later by Zeldovich based on studies of adiabatic flame balls [4]. A diffusion-controlled stationary flame ball with a characteristic equilibrium radius – the flame ball radius – was found to exist via asymptotic analysis [4]. However, stability analysis [8] showed that adiabatic flame balls were inherently unstable: a small perturbation would cause the flame either to propagate inwardly and eventually extinguish, or to propagate outwardly and evolve into a planar flame. The unstable equilibrium flame ball radius (instead of the flame thickness) was therefore considered to be the critical length controlling spherical flame initiation such that the MIE was proposed to be proportional to the cube of the flame ball radius [4–6].

Recently, He [9] studied mixtures with larger Lewis numbers and found that a quasi-steady propagating spherical flame with radius less than the flame ball radius can exist when the Lewis number is sufficiently large. It was concluded that flame initiation for mixtures with large Lewis numbers was controlled not by the radius of stationary flame ball but instead by a minimum flame radius for the existence of self-sustained propagating spherical flames. However, the relation between the minimum ignition energy and the critical ignition length

scale was not examined, and the radiative loss effect was not considered in Ref. [9]. When radiation was included [10], similar results were also found even for mixtures with Lewis number near unity, and the minimum ignition energy was shown to be strongly affected by Lewis number for both adiabatic and non-adiabatic cases.

The discussion above suggests that it is necessary to understand the controlling length scale (the critical flame radius) for spherical flame initiation in order to rigorously determine the minimum ignition energy. Furthermore, since MIE was found to be strongly affected by the Lewis number [11], the effect of preferential diffusion of heat and mass transfer must also be examined. Thus, the objective of the current study is to address the following questions: (1) is the critical flame radius that controls spherical flame initiation the same as the flame thickness or the flame ball radius, (2) how is the critical flame radius related to the flame thickness and flame ball radius if they are not the same, (3) how is the critical flame radius related to the MIE, and (4) how does preferential diffusion of heat and mass affect the critical flame radius as well as the MIE? Below, we first provide a summary of theoretical results so as to provide a unified interpretation of the role of critical flame radius and the effect of preferential diffusion on spherical flame initiation. This is followed by detailed numerical simulations of transient spherical flame initiations of different fuel/oxygen/helium/argon mixtures (fuel: hydrogen, methane, and propane) to demonstrate the validity of the theoretical results.

2. Theoretical analysis

In our previous study [10], spherical flame kernel evolution (with and without an external ignition source at the center) was investigated analytically based on the quasi-steady assumption of flame propagation in the flame-front attached coordinate. The theory developed in Ref. [10] will be utilized here with the main results briefly summarized below.

For adiabatic propagating spherical flames, the following algebraic system of equations for flame propagating speed U (normalized by adiabatic planar flame speed), flame radius R (normalized by adiabatic planar flame thickness), and flame temperature T_f (normalized by adiabatic flame temperature increase) is obtained [10]:

$$\frac{T_f R^{-2} e^{-UR}}{\int_R^\infty \tau^{-2} e^{-U\tau} d\tau} - Q \cdot R^{-2} e^{-UR} = \frac{1}{Le} \frac{R^{-2} e^{-ULeR}}{\int_R^\infty \tau^{-2} e^{-ULe\tau} d\tau}$$
$$= \exp\left[\frac{Z}{2} \frac{T_f - 1}{\sigma + (1-\sigma)T_f}\right], \quad (1)$$

where Le, Z and σ are, respectively, the Lewis number, Zeldovich number, and the ratio of

burned to unburned gas densities [10]. The ignition power is provided as a heat flux at the center [10]. (Steady-state energy deposition is employed in order to achieve an analytical solution. Otherwise, an analytical solution cannot be obtained [10]. However, as will be demonstrated by the numerical results, this simplification is effective to gain qualitative understanding of the physics in a broad parameter range.) By solving Eq. (1) numerically, the relations for the flame propagating speed, flame radius, and flame temperature, as well as the existence of different flame regimes for different Lewis numbers and/or ignition powers can be obtained [10]. It should be noted that the effects of radiative loss [10,12,13] are not considered in this study but are part of our intended future work. In the following, the critical flame radius, the minimum ignition power, and the effects of preferential diffusion will be investigated based on Eq. (1).

As suggested in Refs. [5–9], the critical conditions for a spherical flame to propagate in a self-sustained manner control the spherical flame initiation. Therefore, the conditions for the existence of a propagating spherical flame are first investigated for cases without ignition power deposition at the center ($Q = 0$). Figure 1 shows the flame propagating speed as a function of flame radius for mixtures with different Lewis numbers and $Q = 0$. The Zeldovich number, $Z = 10$, and the thermal expansion ratio, $\sigma = 0.15$, are fixed for all the theoretical results except those in Fig. 5. It is seen that for each mixture at a given Lewis number, there is a critical flame radius, R_C, above which the flame can successfully propagate outward and eventually become a planar flame. On the other hand, there exists no quasi-steady solution below the critical flame radius. Therefore, to successfully initiate a spherical

flame, the ignition source must be large enough to sustain a flame to a radius beyond R_C. The critical radius is shown to increase significantly with the Lewis number. This is due to the fact that the positive stretch rate (proportional to the inverse of flame radius) of the propagating spherical flame makes the flame weaker at higher Lewis numbers [14,15].

The flame ball radius (R_Z, corresponding to $U = 0$ in Fig. 1) was commonly considered to be the minimum radius below which a spherical flame cannot propagate outwards in a self-sustained manner [5,6,8]. However, Fig. 1 shows that R_C is equal to R_Z only when $Le < 1.36$, and that $R_C < R_Z$ for $Le > 1.36$. Therefore, for mixtures with Lewis numbers larger than a critical Lewis number $Le^* = 1.36$, the stationary flame ball radius, R_Z, is not the minimum radius for the existence of propagating spherical flames, and the critical flame radius controlling spherical flame initiation is neither the stationary flame ball radius nor the flame thickness.

We now consider cases in which an external energy flux is deposited in the center of a quiescent mixture and examine how the ignition power correlates with the critical flame radius. Figure 2 shows the flame propagating speed as a function of flame radius at different ignition powers for mixtures with $Le = 2$. For $Q = 0$, only a C shaped flame branch for U–R exists (which is also shown in Fig. 1 for $Le > Le^* = 1.36$), and there is a critical flame radius, R_C, at the turning point, and a flame ball radius, R_Z, at $U = 0$. At a low ignition power, $Q = 0.5$, there is a new flame branch (left branch) of U–R solution curve at small flame radii with the flame propagating speed decreasing sharply to zero (flame ball solution). On the left branch, the maximum possible flame radius is defined as the lower critical flame radius, R_C^-, and the flame ball solution is defined as the lower flame ball radius, R_Z^-. It is seen that $R_C^- = R_Z^-$ for $Q = 0.5$. The C shaped flame branch (right branch) is shown to be slightly shifted to the left side due to the ignition power deposition. On the right branch, the corresponding upper critical flame radius, R_C^+, and the upper flame ball radius, R_Z^+ are defined in the opposite way. It is seen that the left and right branches move towards each other when the ignition power increases. When the ignition power is larger than a critical value (equal to 0.968 for $Le = 2$), the two branches merge with each other, resulting in new upper and lower branches. A spherical flame can thereafter propagate outward along the upper branch U–R correlation and a successful spherical flame initiation can be achieved. Therefore, this critical ignition power is defined as the minimum ignition power, Q_{min}. It should be noted that Fig. 2 shows that there might be two flame propagating speed solutions for a given flame radius and ignition power. However, the fast flame speed solution is stable while the slow one is unstable, which
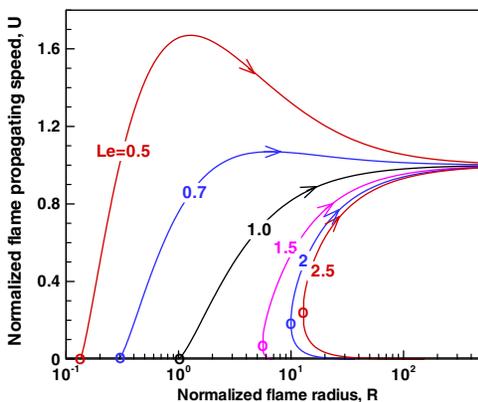

Fig. 1. Flame speed as a function of flame radius for mixtures with different Lewis numbers and $Q = 0$ (the critical flame radius for each case is denoted by a circle at the corresponding minimum flame radius).
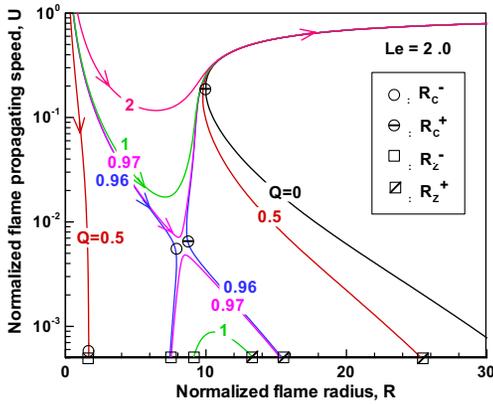
Fig. 2. Normalized flame propagating speed as a function of flame radius at different ignition powers.

corresponds to an unrealistic solution from theoretical analysis and thus cannot be realized by numerical simulation [10].

The changes of the upper and lower critical flame radii and flame ball radii with the ignition power are shown in Fig. 3 for $Le = 2.5$ as well as $Le = 2.0$. It is observed that the upper and lower flame ball radii, R_Z^+ and R_Z^-, are both strongly affected by the ignition power. However, for the critical flame radii, R_C^- monotonically increases with Q, while R_C^+ remains almost constant. The lower critical flame radius and the lower flame ball radius are shown to be almost the same ($R_C^- \approx R_Z^-$). According to the definition of Q_{min} given above, the minimum ignition power for successful flame initiation is reached when $R_C^+ = R_C^-$ (denoted by the dashed lines in Fig. 3). In Refs. [5,6,8], the minimum ignition power is defined as the power at which $R_Z^+ = R_Z^-$. Figure 3 shows that the minimum ignition power defined according to $R_Z^+ = R_Z^-$ ($Q'_{min} = 1.048$ for Le = 2 and $Q'_{min} = 2.53$ for $Le = 2.5$) is higher
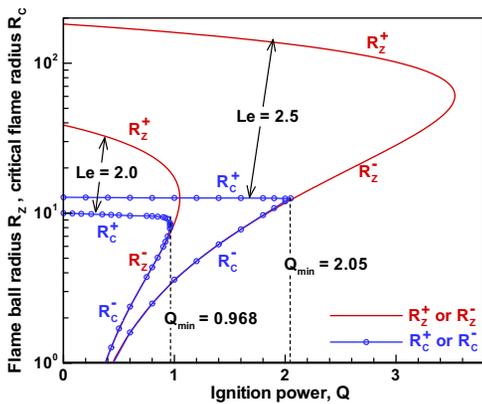
than the Q_{min} defined based on the critical flame radius ($Q_{min} = 0.968$ for $Le = 2$ and $Q_{min} = 2.05$ for $Le = 2.5$). Therefore, for mixtures with Lewis numbers larger than the critical Lewis number, $Le^* = 1.36$, the minimum ignition power is over-predicted based on the flame ball radius. Only for mixtures with Lewis number less than $Le^* = 1.36$ is the minimum ignition power based on the critical flame radius the same as that based on the flame ball radius.

It is noted that the critical flame radius, $R_C^+ = R_C^-$, at the minimum ignition power, is nearly the same as the critical flame radius, R_C, at zero ignition power deposition since R_C^+ remains almost constant for different Q (Fig. 3). Comparing the critical flame radius and the flame ball radius at $Q = 0$ reveals that the minimum ignition power is over-predicted using the flame ball radius instead of the critical flame radius. Figure 4 shows the variation of the critical flame radius and the flame ball radius (both normalized by the flame thickness) with Lewis number. They are both shown to depend strongly on the Lewis number. Three different regimes in terms of the Lewis number are observed. In regimes I and II, with Lewis number less than $Le^* = 1.36$, the critical flame radius is the same as the flame ball radius and it is smaller/larger than the flame thickness when the Lewis number is below unity (regime I)/ above unity (regime II). In regime III, with $Le > Le^*$, the critical flame radius is shown to be smaller than the flame ball radius but larger than the flame thickness. The difference between the critical flame radius and the flame ball radius/flame thickness is of order-one magnitude when $Le > 2.0$. As a result, the minimum ignition power will be substantially over-predicted/under-predicted based on the flame ball radius/flame thickness for mixtures with large Lewis numbers. Therefore, the flame ball radius can be considered as the flame initiation controlling length only for mixtures with $Le < Le^*$ while the flame thickness only for $Le = 1.0$.

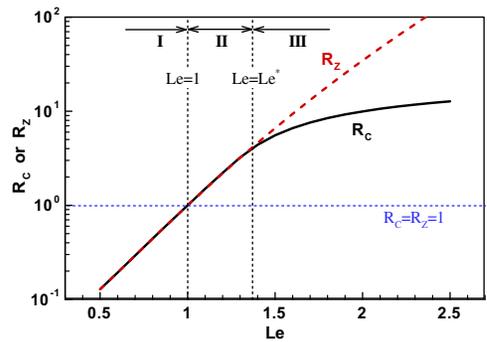Fig. 3. Change of upper and lower critical flame radii and flame ball radii with the ignition power.

Fig. 4. Change of the critical flame radius and the flame ball radius with the Lewis number.

To reveal the correlation between Q_{min} and R_C, the minimum ignition power, Q_{min}, and the cube of the critical flame radius, R_C^3, for mixtures with different Lewis numbers ($Le = 1.4$–2.5) and Zeldovich numbers ($Z = 10$, 13) are plotted in Fig. 5. Both Q_{min} and R_C^3 are shown to depend strongly on the Lewis number. Moreover, it is observed that the minimum ignition power varies almost linearly with the cube of the critical flame radius, i.e. $Q_{min} \sim R_C^3$. Therefore, the minimum energy deposition for successful spherical flame initiation is proportional to the cube of the critical flame radius. If the minimum ignition power is plotted against the cube of flame ball radius or flame thickness, the correlation would not be linear since the flame ball radius/flame thickness is much larger/smaller than the critical flame radius when $Le > Le^* = 1.36$.

The above results show that the relationship among the critical flame radius, the flame ball radius, and the flame thickness strongly depends on the Lewis number and that the minimum ignition power varies almost linearly with the cube of the critical flame radius. These results were obtained from theoretical analysis. One limitation of this analysis is that the ignition energy deposition is modeled as a boundary condition in the center [10]; under most realistic conditions, it is deposited as a function of time and space. Moreover, the theoretical analysis is constrained by quasi-steady, constant-density, and infinite activation energy assumptions. In the next section, we present results from direct numerical simulations (with detailed chemistry) that include all of the above-mentioned effects neglected in the theoretical analysis in order to test the applicability of the theoretical results under more realistic conditions. As shown below, the simulations qualitatively confirm the results obtained from the theoretical analysis.
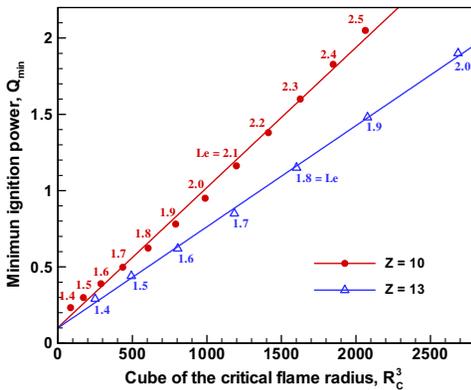

Fig. 5. Minimum ignition power and cube of the critical flame radius for mixtures with different Lewis numbers and Zeldovich numbers.

3. Numerical simulation

A time-accurate and space-adaptive numerical solver for Adaptive Simulation of Unsteady Reacting Flow, A-SURF, has been developed [19] and used to study spherical flame initiation and propagation. The conservation equations of one-dimensional, compressible, multi-component-diffusive, reactive flow in a spherical coordinate are solved using the finite volume method [16,19]. The convective flux, diffusion flux, and stiff chemistry are calculated by MUSCL-Hancock scheme, central difference scheme, and VODE solver, respectively [16,19]. The thermodynamic and transport properties as well as the chemical reaction rates are evaluated by CHEMKIN packages [17] incorporated into A-SURF. A-SURF has been successfully used in our previous studies on propagating spherical flames [18–22]. The details on the governing equations, numerical schemes, and code validation can be found in Refs. [16,19].

In all the simulations, the computational domain is $0 \leqslant r \leqslant 100$ cm and a multi-level, dynamically adaptive mesh [16,19] with a minimum mesh size of 8 μm is used. Zero-gradient conditions are enforced at both inner ($r = 0$) and outer ($r = 100$ cm) boundaries. At the initial state, the homogeneous mixture is quiescent at 298 K and atmospheric pressure. Flame initiation is achieved by spatial dependent energy deposition for a given ignition time [23]

$$\dot{q}_{ignit} = \begin{cases} \frac{E}{4\pi r_{ig}^3 \tau_{ig}/3} \exp\left[-\frac{\pi}{4}\left(\frac{r}{r_{ig}}\right)^6\right] & \text{if } t < \tau_{ig} \\ 0 & \text{if } t \geqslant \tau_{ig} \end{cases}$$ (2)

where E is the total ignition energy, τ_{ig}, the duration of the energy source, and r_{ig}, the ignition kernel radius. It is noted that the duration of the source energy and the ignition kernel size both affect the MIE [1,2,24]. In this study, since the emphasis is on the correlation between the MIE and the critical flame radius and on the Lewis number effect on spherical flame initiation, both the ignition kernel size and time are kept constant with $\tau_{ig} = 200$ μs and $r_{ig} = 200$ μm, respectively. The values of τ_{ig} and r_{ig} are chosen according to the simulation results reported in Ref. [23] which presented the dependence of the MIE on the ignition kernel size and time.

Simulations utilizing detailed chemical mechanisms for fuel/O_2/He/Ar mixtures (fuel: H_2, CH_4 and C_3H_8) have been conducted. For H_2/O_2/He/Ar mixtures, the recent mechanism developed by Li et al. [25] is employed. For CH_4/O_2/He/Ar and C_3H_8/O_2/He/Ar mixtures, GRI-MECH 3.0 [26] and San-Diego Mechanism 20051201 [27] are used, respectively. The mixture composition is specified in the form of

$$0.3\left(\frac{\varphi}{\varphi+r_s}\text{Fuel}+\frac{r_s}{\varphi+r_s}\text{O}_2\right)+\alpha\text{He}+(0.7-\alpha)\text{Ar}, \quad (3)$$

where φ is the equivalence ratio and r_s is the stoichiometric oxygen-to-fuel molar ratio ($r_s = 0.5$ for H_2, 2.0 for CH_4, and 5.0 for C_3H_8). The volumetric fraction of fuel and oxygen is fixed to be 30%, while that of inert diluents, helium and argon, is fixed to be 70%. With the increase/decrease of the helium/argon fraction, the thermal diffusivity of the mixture increases, resulting in a higher Lewis number [18] while the global activation energy as well as the adiabatic flame temperature remains nearly unchanged, resulting in the same Zeldovich number. Therefore, different amounts of helium ($\alpha = 0\%$, 25%, 50% and 70%) can be used here to investigate the Lewis number effect on spherical flame initiation.

Figure 6 shows the flame radius evolution for different ignition energies for $H_2/O_2/He/Ar$ at $\varphi = 2.0$ and $\alpha = 0\%$. The MIE for this mixture, $E_{min} = 0.165$ mJ, and for all other mixtures was calculated by the method of trial-and-error with relative error below 2%. It is observed that a self-sustained propagating flame can be successfully initiated only when the ignition energy is above the MIE. By plotting the flame propagating speed, $S_b = dR_f/dt$, as a function of flame radius, results (not shown here due to space limitation) similar to the theoretical predictions shown in Fig. 2 (except the right and lower branches which cannot be calculated from transient numerical simulation) are obtained. In the numerical simulation, the critical flame radius cannot be defined in the same way as that in the quasi-steady theoretical analysis. However, Fig. 2 shows that the critical flame radius is almost the same as the flame radius at which the minimum propagating speed occurs with the minimum ignition power deposition ($Q = 0.97$). Therefore, the critical flame

radius in the transient numerical simulations is defined as the radius corresponding to the minimum propagating speed for MIE deposition. A similar definition was also used in experimental measurements [7]. In Fig. 6, the critical flame radius, $R_C = 0.11$ cm, occurs at the inflection point for $E = E_{min} = 0.165$ mJ.

To investigate the preferential diffusion effect on spherical flame initiation, numerical simulations on the initiation of $H_2/O_2/He/Ar$ flames at different equivalence ratios and different amounts of helium dilutions were conducted. The burned Markstein length (L_b), the critical flame radius (R_C), and the MIE (E_{min}) of different $H_2/O_2/He/Ar$ mixtures are shown in Fig. 7. The burned Markstein length, L_b, is obtained from linear regression of the flame propagating speed, $S_b = dR_f/dt$, and the flame stretch rate, $K = (2/R_f)(dR_f/dt)$ [15,21,22]. Figure 7a shows that the burned Markstein length increases with the helium fraction at each equivalence ratio. It is well known that the burned Markstein length increases with the Lewis number [14,15]. Therefore, as mentioned before, the Lewis number also increases with helium fraction. Figure 7a also shows that the burned Markstein length increases with the equivalence ratio for a fixed helium fraction. Therefore, the Lewis number of the $H_2/O_2/He/Ar$ mixture increases with both the helium fraction and the equivalence ratio. Consistent with

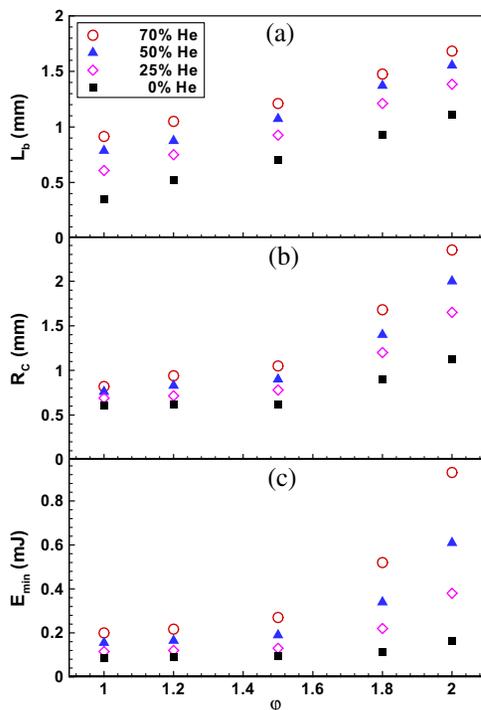Fig. 6. Spherical flame initiation for $H_2/O_2/Ar$ mixtures at different ignition energies.

Fig. 7. Burned Markstein length (a), critical flame radius (b), and minimum ignition energy (c) of $H_2/O_2/He/Ar$ mixtures.

the theoretical analysis on the Lewis number effect (Fig. 5), Fig. 7b and c show that the critical flame radius and the MIE of the $H_2/O_2/He/Ar$ mixtures also increase with the helium fraction and the equivalence ratio. These results are also consistent with previous studies on the Lewis number effect on the critical flame radius [7] and the MIE [11].

To reveal how the critical flame radius is correlated with the MIE, Fig. 8 shows the MIE as a function of the cube of the critical flame radius for $H_2/O_2/He/Ar$ mixtures with different equivalence ratios and different helium fractions. Similar to the theoretical results (Fig. 5), the transient numerical simulation also shows that the MIE changes almost linearly with the cube of critical flame radius instead of the flame thickness or the flame ball radius, demonstrating a linear correlation: $E_{min} \sim R_C^3$. Therefore, the linear dependence of the MIE on the cube of the critical flame radius reveals that the critical flame radius defined in this study is the controlling length scale for spherical flame initiation and the MIE. Figure 8 also shows that the slope of E_{min}–R_C^3 decreases with the increase of the equivalence ratio. This is because the activation energy increases while the adiabatic flame temperature decreases with the equivalence ratio for rich $H_2/O_2/He/Ar$ flames, which results in a larger Zeldovich number at higher equivalence ratio. Therefore the numerical simulation demonstrates that the slope of E_{min}–R_C^3 decreases with the Zeldovich number, which is the same as the conclusion drawn from the theoretical analysis (see Fig. 5). As discussed above, the ignition energy is specified differently in theory and simulation – it is given as a boundary condition at the center in the theoretical analysis and as a volumetric, time-dependent heat source in the simulation. Therefore, the comparison between the theoretical and numerical results yields qualitative instead of quantitative agreement.
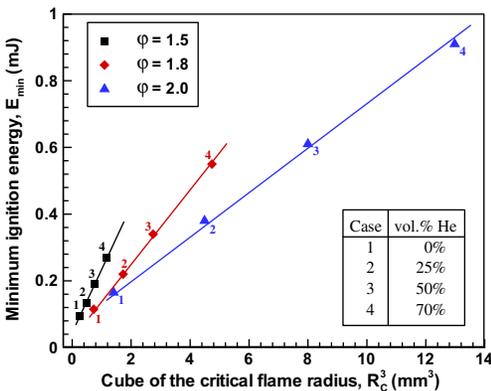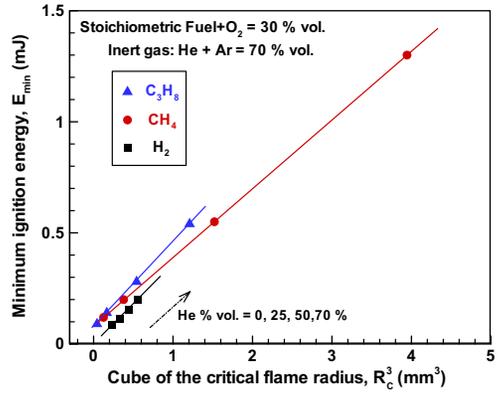

Fig. 9. Minimum ignition energy and cube of the critical flame radius of different fuel/O_2/He/Ar mixtures.

To further demonstrate the validity of the theoretical results, simulations for other fuels (CH$_4$ and C$_3$H$_8$) have also been conducted. Similar results to those of $H_2/O_2/He/Ar$ are obtained. Figure 9 shows that the linear correlation, $E_{min} \sim R_C^3$, also works for $CH_4/O_2/He/Ar$ and $C_3H_8/O_2/He/Ar$ mixtures. Therefore, the numerical simulation demonstrates the validity of the theoretical results in that the MIE is proportional to the cube of the critical flame radius instead of the flame thickness or the flame ball radius.

4. Concluding remarks

Spherical flame initiation is studied using asymptotic analysis and detailed numerical simulations. The critical flame radius that controls spherical flame initiation is found to be different from the flame thickness and the flame ball radius. Depending on the Lewis number, there are three different flame initiation regimes: in regime I with $Le < 1.0$, the critical flame radius and the flame ball radius are the same and are smaller than the flame thickness; in regime II with $1.0 < Le < Le^*$, the critical flame radius and the flame ball radius are also the same but are larger than the flame thickness; while in regime III with $Le > Le^*$, the critical flame radius is smaller than the flame ball radius but larger than the flame thickness. Therefore, the minimum ignition energy can be substantially over-predicted (under-predicted) based on the flame ball radius (the flame thickness) for mixtures with large Lewis numbers. A linear relationship between the minimum ignition energy/power and the cube of the critical flame radius is demonstrated by both theory and simulation. Moreover, the Lewis number effect is shown to play a very important role in spherical flame initiation. The critical flame radius and the minimum ignition energy increase significantly with the Lewis

Fig. 8. Minimum ignition energy and cube of the critical flame radius of different $H_2/O_2/He/Ar$ mixtures.

number. Therefore, for fuels with much higher thermal diffusivity than fuel mass diffusivity, larger ignition energy is needed to initiate a self-sustained propagating premixed flame.

In previous experimental studies on the MIE in the literature (see Ref. [1] and references therein), not only the Lewis number but also the global activation energy and the flame temperature varied with mixture composition. Therefore, those data cannot be used to demonstrate directly the effects of Lewis number on the ignition and the linear correlation between MIE and the cube of the critical flame radius (Figs. 5, 8 and 9 show that the linear correlation depends on the activation energy). Nevertheless, the experimental data [28] showed that for lean mixtures, the MIE increases dramatically from methane to ethane, propane and butane, which is consistent to the present results of the effect of the Lewis number. In order to further validate the theoretical results in this study by experiments, measurements of the MIE and critical flame radius of different fuel/O_2/He/ Ar mixtures should be conducted, for which the Lewis number can be modified by varying the helium/argon fraction such that the global activation energy as well as the adiabatic flame temperature remain nearly unchanged.

Acknowledgements

References

[1] P.D. Ronney, *Opt. Eng.* 33 (1994) 510–521.

[2] B. Lewis, G. Von Elbe, *Combustion Flames and Explosive of Gases*, Academic Press, New York, 1961.

[3] F.A. Williams, *Combustion Theory*, Benjamin-Cummins, Menlo Park, CA, 1985.

[4] Y.B. Zeldovich, G.I. Barenblatt, V.B. Librovich, G.M. Makhviladze, *The Mathematical Theory of Combustion and Explosions*, Consultants Bureau, New York, 1985.

[5] M. Champion, B. Deshaies, G. Joulin, K. Kinoshita, *Combust. Flame* 65 (1986) 319–337.

[6] Y. Ko, R.W. Anderson, V.S. Arpaci, *Combust. Flame* 83 (1991) 75–87.

[7] A.P. Kelley, G. Jomaas, C.K. Law, *Combust. Flame* 156 (2009) 1006–1013.

[8] B. Deshaies, G. Joulin, *Combust. Sci. Technol.* 37 (1984) 99–116.

[9] L. He, *Combust. Theor. Model.* 4 (2000) 159–172.

[10] Z. Chen, Y. Ju, *Combust. Theor. Model.* 11 (2007) 427–453.

[11] P.S. Tromans, R.M. Furzeland, *Proc. Combust. Inst.* 21 (1988) 1891–1897.

[12] Z. Chen, Y. Ju, *Int. J. Heat Mass Transfer* 51 (2008) 6118–6125.

[13] Z. Chen, X. Gou, Y. Ju, *Combust. Sci. Technol.* 182 (2010) 124–142.

[14] C.K. Law, *Combustion Physics*, Cambridge University Press, 2006.

[15] P. Clavin, *Prog. Energy Combust. Sci.* 11 (1985) 1–59.

[16] Z. Chen, *Combust. Flame* (2010), doi:10.1016/j.combustflame.2010.07.010.

[17] R.J. Kee, F.M. Rupley, J.A. Miller, Report SAND89-8009B, Sandia National Laboratory, 1989.

[18] Z. Chen, X. Qin, B. Xu, Y. Ju, F. Liu, *Proc. Combust. Inst.* 31 (2007) 2693–2700.

[19] Z. Chen, M.P. Burke, Y. Ju, *Proc. Combust. Inst.* 32 (2009) 1253–1260.

[20] M.P. Burke, Z. Chen, Y. Ju, F.L. Dryer, *Combust. Flame* 156 (2009) 771–779.

[21] Z. Chen, M.P. Burke, Y. Ju, *Combust. Theor. Model.* 13 (2009) 343–364.

[22] Z. Chen, *Int. J. Hydrogen Energy* 34 (2009) 6558–6567.

[23] A. Frendi, M. Sibulkin, *Combust. Sci. Technol.* 73 (1990) 395–413.

[24] T.M. Sloane, P.D. Ronney, *Combust. Sci. Technol.* 88 (1993) 1–13.

[25] J. Li, Z.W. Zhao, A. Kazakov, F.L. Dryer, *Int. J. Chem. Kinet.* 36 (2004) 566–575.

[26] G.P. Smith, et al., Available from: <http://www.me.berkeley.edu/gri_mech/>.

[27] F.A. Williams, Available from: <http://mae-web.ucsd.edu/~combustion/>.

[28] R.K.R.K. Eckhoff, *Explosion Hazards in the Process Industries*, Gulf Publishing Company, Houston, 2005.

[29] U. Mass, J. Warnatz, *Combust. Flame* 74 (1988) 53–69.

[30] H.J. Kim, S.H. Chung, C.H. Sohn, *KSME Int. J.* 18 (2004) 838–846.